

## Factors Affecting Gas-Phase Deuterium Scrambling in Peptide Ions and Their Implications for Protein Structure Determination

Jeroen A. A. Demmers,<sup>†,‡</sup> Dirk T. S. Rijkers,<sup>§</sup> Johan Haverkamp,<sup>†</sup>  
J. Antoinette Killian,<sup>‡</sup> and Albert J. R. Heck<sup>\*,†</sup>

*Contribution from the Department of Biomolecular Mass Spectrometry, Bijvoet Center for Biomolecular Research and Utrecht Institute for Pharmaceutical Sciences, Utrecht University, Sorbonnelaan 16, 3584 CA Utrecht, The Netherlands, Department of Biochemistry of Membranes, Center for Biomembranes and Lipid Enzymology, Institute of Biomembranes, Utrecht University, Padualaan 8, 3584 CH Utrecht, The Netherlands, and Department of Medicinal Chemistry, Utrecht Institute for Pharmaceutical Sciences, Utrecht University, Sorbonnelaan 16, 3584 CA Utrecht, The Netherlands*

Received November 26, 2001

**Abstract:** In this report, we evaluate the validity of using hydrogen/deuterium exchange in combination with collision-induced dissociation mass spectrometry (CID MS) for the detailed structural and conformational investigation of peptides and proteins. This methodology, in which partly deuterated peptide ions are subjected to collision-induced dissociation in the vacuum of a mass spectrometer, has emerged as a useful tool in structural biology. It may potentially provide quantitatively the extent of deuterium incorporation per individual amino acid in peptides and proteins, thus providing detailed structural information related to protein structure and folding. We report that this general methodology has limitations caused by the fact that the incorporated deuterium atoms migrate prior or during the CID MS analysis. Our data are focused on a variety of transmembrane peptides, incorporated in a lipid bilayer, in which the near-terminal amino acids that anchor at the lipid–water interface are systematically varied. Our findings suggest that, under the experimental conditions we use, the extent of intramolecular hydrogen scrambling is strongly influenced by experimental factors, such as the exact amino acid sequence of the peptide, the nature of the charge carrier, and therefore most likely by the gas-phase structure of the peptide ion. Moreover, the observed scrambling seems to be independent of the nature of the peptide fragment ions (i.e., protonated B and Y' ions, and sodiated A and Y' ions). Our results strongly suggest that scrambling may be reduced by using alkali metal cationization instead of protonation in the ionization process.

### Introduction

Solution-phase hydrogen/deuterium (H/D) exchange in combination with electrospray ionization mass spectrometry (ESI-MS) has become a useful tool to study protein structure and conformation,<sup>1–6</sup> protein–protein interactions, and protein–membrane interfacial regions.<sup>7–10</sup> By determination of mass

increases because of the uptake of deuterium atoms in time, global exchange kinetics can be derived. To reveal the sites of deuterium incorporation at a higher resolution, the protein can be cleaved enzymatically, and the resulting peptides can subsequently be fragmented by gas-phase collision-induced dissociation (CID) to get isotopic information. However, interpretation of CID MS data on partly deuterated peptide ions can, in principle, be hampered by both inter- and intramolecular migration of hydrogens, that is, deuteriums. Obviously, for detailed structural analysis both migration processes are undesirable and need to be addressed in detail.

Intermolecular exchange can take place when peptide ions in the gas phase undergo collisions with gaseous H<sub>2</sub>O or D<sub>2</sub>O in the relatively high-pressure region at the interface. Such bimolecular H/D exchange reactions of peptides and proteins in the gas phase have been studied extensively (e.g., refs 11–14), and exchange rates have been proposed to be dependent on a number of factors, like gas-phase proton affinity, acces-

\* To whom correspondence should be addressed. E-mail: a.j.r.heck@chem.uu.nl.

<sup>†</sup> Department of Biomolecular Mass Spectrometry, Utrecht University.

<sup>‡</sup> Department of Biochemistry of Membranes, Utrecht University.

<sup>§</sup> Department of Medicinal Chemistry, Utrecht University.

(1) Smith, D. L.; Deng, Y.; Zhang, Z. *J. Mass Spectrom.* **1997**, *32*, 135–46.

(2) Engen, J. R.; Smith, D. L. *Anal. Chem.* **2001**, *73*, 256A–65A.

(3) Tito, P.; Nettleton, E. J.; Robinson, C. V. *J. Mol. Biol.* **2000**, *303*, 267–78.

(4) Wood, T. D.; Chorush, R. A.; Wampler, F. M., III; Little, D. P.; O'Connor, P. B.; McLafferty, F. W. *Proc. Natl. Acad. Sci. U.S.A.* **1995**, *92*, 2451–4.

(5) Maier, C. S.; Schimerlik, M. I.; Deinzer, M. L. *Biochemistry* **1999**, *38*, 1136–43.

(6) Wagner, D. S.; Melton, L. G.; Yan, Y.; Erickson, B. W.; Anderegg, R. J. *Protein Sci.* **1994**, *3*, 1305–14.

(7) Mandell, J. G.; Baerga-Ortiz, A.; Akashi, S.; Takio, K.; Komives, E. A. *J. Mol. Biol.* **2001**, *306*, 575–89.

(8) Akashi, S.; Takio, K. *Protein Sci.* **2000**, *9*, 2497–505.

(9) Demmers, J. A. A.; Haverkamp, J.; Heck, A. J. R.; Koeppe, R. E., II; Killian, J. A. *Proc. Natl. Acad. Sci. U.S.A.* **2000**, *97*, 3189–194.

(10) Demmers, J. A. A.; van Duijn, E.; Haverkamp, J.; Greathouse, D. V.; Koeppe, R. E., II; Heck, A. J. R.; Killian, J. A. *J. Biol. Chem.* **2001**, *276*, 34501–8.

sibility of exchangeable sites at the surface, and the structure of the molecule.

In addition, isotopic information can be depleted by intramolecular migration of hydrogens or deuteriums (a process also referred to as “scrambling”), which involves the redistribution of hydrogen isotopes over the peptide ion as a consequence of high hydrogen mobility. Under what conditions the process of hydrogen migration within peptides takes place is not fully understood.<sup>15,16</sup> It may be that scrambling occurs induced by the numerous collisions with neutral gas molecules during the collisional activation and, therefore, would be a direct consequence of the peptide fragmentation process. Alternatively, it could be that scrambling occurs earlier in the analysis process, for example, somewhere during the ionization process or between the ionization and collisional activation.

In the literature, conflicting results have been reported about scrambling in peptide ions. In several studies, it has been shown that hydrogen mobility within peptide ions is sufficiently rapid to scramble their position even prior to collisional activation,<sup>11,17,18</sup> whereas in other studies, it has been claimed that intramolecular migration of amide hydrogens is minor or even negligible.<sup>8,10,16,19–22</sup> As H/D exchange in combination with CID MS is used more and more for structural and conformational investigations of proteins and peptides, it is very important to understand the factors underlying deuterium scrambling and to find ways to control or prevent this process.

In our research, we aim to use H/D exchange in combination with CID MS to study in detail the structural interactions of transmembrane proteins and peptides within the membrane. We showed before<sup>9,10</sup> that H/D exchange in hydrophobic transmembrane peptides can be measured by mass spectrometry by direct introduction of these (normally insoluble) peptides using vesicular structures of phospholipid bilayers dispersed in aqueous buffer. To obtain more detailed information on the architecture of the transmembrane peptides in the bilayer, we performed CID MS experiments on the partly deuterated peptides.<sup>9,10</sup> In these previous studies, no significant amount of deuterium scrambling was observed, which allowed us to determine the nature of peptide–model membrane interactions. However, in these experiments, only transmembrane peptides consisting of a Leu-Ala sequence of variable length and flanked by Trp residues were used. Because these peptides could hardly be protonated because of their hydrophobicity and lack of charged residues, all experiments in these previous studies were performed on sodiated peptide species. To test whether this CID MS-based method is also valid for protonated peptide species,

as well as for peptides containing different flanking residues, we decided to address this issue in more detail. The goal of the present study was therefore to systematically investigate the possible occurrence of deuterium scrambling and to elucidate the influence of several crucial experimental factors on scrambling during CID MS.

In our experiments, we make use of peptides with a general acetyl-GX<sub>2</sub>(LA)<sub>n</sub>LX<sub>2</sub>A-ethanolamine/amide sequence (where X is a variable residue and  $n = 7$  or  $8$ ), which are incorporated in phospholipid bilayers in an  $\alpha$ -helical manner and in a transmembrane orientation, as verified by oriented circular dichroism, polarized Fourier transform infrared spectroscopy, and nuclear magnetic resonance spectroscopy measurements.<sup>23–25</sup> All experiments were performed at neutral pH. Both the protonated and the sodium-cationized species were then subjected to CID MS. This system is very suitable to study the extent of deuterium scrambling during CID MS for several reasons. First, the time window in which the peptides remain only partly deuterated is very long as the exchange rates in the hydrophobic core of the peptide are extremely low in contrast with water-soluble peptides of similar length.<sup>9,10</sup> As a consequence, it is possible to perform CID MS experiments on the full length peptides at time points when the deuterium content is relatively constant with respect to the time it takes to perform such an experiment. Consequently, there is no need for lowering the pH to quench H/D exchange, which might introduce unwanted side effects. Second, as we may get full sequence coverage over the transmembrane peptides in the CID MS fragmentations, there is no need for prior digestion of the protein into smaller peptides, which may complicate the interpretation of the data. Finally, a set of transmembrane peptides is available, which vary only in the near-terminal amino acid residues. The hydrophobic core and the terminal residues are kept invariant. Because of these reasons, we believe that this experimental system provides a unique opportunity to study the influence of specific factors on the extent of scrambling.

## Materials and Methods

**Chemicals.** The peptides WALP21, WALP23, KALP23, HALP23, FALP21, and YALP21 (see Table 1) were synthesized as described previously.<sup>23,24</sup> K\*ALP23 (see Table 1) was obtained by reductive methylation of KALP23. Reductive methylation was performed using a modified procedure based on previously published methods.<sup>26,27</sup> Briefly, 10  $\mu$ mol of KALP23 peptide was dissolved in 25 mL of dioxane/methanol/0.6 M NaHCO<sub>3</sub> (14:5:1, v/v/v), and the pH was raised by addition of 100  $\mu$ L of a 20 g NaOH/L solution. Subsequently, 320  $\mu$ mol of 37% formaldehyde diluted with dioxane/methanol (1:1, v/v) was added, giving an 8-fold excess of formaldehyde over the numbers of lysine residues present. NaBH<sub>3</sub>CN dissolved in acetonitrile/water (1:1, v/v) was added in small portions to a final concentration of 20 mM. The reaction mixture was stirred for 18 h at room temperature. The identity of the peptide after methylation was determined by ESI MS/MS, which showed that each of the lysine side-chain nitrogens was dimethylated.

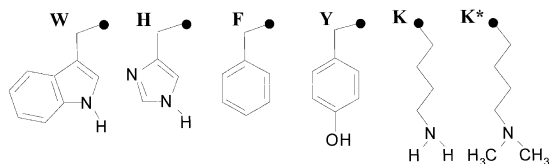
- (11) McLafferty, F. W.; Guan, Z. Q.; Hapts, U.; Wood, T. D.; Kelleher, N. L. *J. Am. Chem. Soc.* **1998**, *120*, 4732–40.
- (12) Cassady, C. J. *J. Am. Soc. Mass Spectrom.* **1998**, *9*, 716–23.
- (13) Kaltashov, I. A.; Doroshenko, V. M.; Cotter, R. J. *Proteins* **1997**, *28*, 53–8.
- (14) Heck, A. J. R.; Jorgensen, T. J. D.; O'Sullivan, M.; von Raumer, M.; Derrick, P. J. *J. Am. Soc. Mass Spectrom.* **1998**, *9*, 1255–66.
- (15) Buijs, J.; Hagman, C.; Hakansson, K.; Richter, J. H.; Hakansson, P.; Oscarsson, S. *J. Am. Soc. Mass Spectrom.* **2001**, *12*, 410–9.
- (16) Deng, Y. Z.; Pan, H.; Smith, D. L. *J. Am. Chem. Soc.* **1999**, *121*, 1966–7.
- (17) Harrison, A. G.; Yalcin, T. *Int. J. Mass Spectrom.* **1997**, *165*, 339–47.
- (18) Johnson, R. S.; Krylov, D.; Walsh, K. A. *J. Mass Spectrom.* **1995**, *30*, 386–7.
- (19) Eyles, S. J.; Speir, J. P.; Kruppa, G. H.; Gierasch, L. M.; Kaltashov, I. A. *J. Am. Chem. Soc.* **2000**, *122*, 495–500.
- (20) Akashi, S.; Naito, Y.; Takio, K. *Anal. Chem.* **1999**, *71*, 4974–80.
- (21) Anderegg, R. J.; Wagner, D. S.; Stevenson, C. L.; Borchardt, R. T. *J. Am. Soc. Mass Spectrom.* **1994**, *5*, 425–33.
- (22) Kim, M. Y.; Maier, C. S.; Reed, D. J.; Deinzer, M. L. *J. Am. Chem. Soc.* **2001**, *123*, 9860–6.

- (23) Killian, J. A.; Saleminck, I.; de Planque, M. R.; Lindblom, G.; Koepp, R. E., II; Greathouse, D. V. *Biochemistry* **1996**, *35*, 1037–45.
- (24) de Planque, M. R. R.; Kruijtzter, J. A. W.; Liskamp, R. M. J.; Marsh, D.; Greathouse, D. V.; Koepp, R. E., II; de Kruijff, B.; Killian, J. A. *J. Biol. Chem.* **1999**, *274*, 20839–46.
- (25) de Planque, M. R. R.; Goormaghtigh, E.; Greathouse, D. V.; Koepp, R. E., II; Kruijtzter, J. A. W.; Liskamp, R. M. J.; de Kruijff, B.; Killian, J. A. *Biochemistry* **2001**, *40*, 5000–10.
- (26) Jentoft, N.; Dearborn, D. G. *J. Biol. Chem.* **1979**, *254*, 4359–65.
- (27) Dottavio-Martin, D.; Ravel, J. M. *Anal. Biochem.* **1978**, *87*, 562–5.

**Table 1.** Sequences of Transmembrane Peptides Used (Variable Flanking Residues Are Bold-Faced)<sup>a</sup>

peptide	sequence
FALP21	Ac-G <b>FF</b> LALALALALALALAL <b>FF</b> A-Am
HALP23	Ac-G <b>HH</b> LALALALALALALALAL <b>HH</b> A-Am
KALP23	Ac-G <b>KK</b> LALALALALALALALAL <b>KK</b> A-Am
K*ALP23	Ac-G <b>K*</b> K*LALALALALALALALAL <b>K*</b> K*A-Am
WALP21	Ac-G <b>WW</b> LALALALALALALAL <b>WW</b> A-Etn
WALP23	Ac-G <b>WW</b> LALALALALALALAL <b>WW</b> A-Etn
YALP21	Ac-G <b>YY</b> LALALALALALALAL <b>YY</b> A-Am

<sup>a</sup> Abbreviations: Ac, acetyl; Am, amide; Etn, ethanolamide; A, alanine; F, phenylalanine; G, glycine; H, histidine; K, lysine; L, leucine; W, tryptophan; Y, tyrosine, K\*, lysine with dimethylated side-chain nitrogen; XALP21, peptide with acetyl-GXX(LA)<sub>7</sub>LXXA-amide sequence (X = F or Y); XALP23, peptide with acetyl-GXX(LA)<sub>8</sub>LXXA-amide/ethanolamine sequence (X = H, K, K\*, or W). For chemical structure of amino acid side chains, see below.



Trifluoroacetic acid (TFA) was obtained from Merck (Darmstadt, Germany), and 2,2,2-trifluoroethanol (TFE) was obtained from Sigma (St. Louis, MO). Deuterium oxide (>99.9% D) was obtained from Aldrich Chemical Co., Inc. (Milwaukee, WI) and was stored under nitrogen at 4 °C. Sodium iodide was from OPG Farma Company (Utrecht, The Netherlands). Ammonium acetate was from Fluka (Switzerland). The phospholipid dimyristoylphosphatidylcholine (DMPC) was obtained from Avanti Polar Lipids Inc. (Birmingham, AL).

**Proteoliposome Preparation.** Peptide incorporation into phospholipid vesicles and ESI MS measurements were performed essentially as described previously.<sup>9,10</sup> Briefly, peptides were dissolved in TFE (1 mg/mL). The peptide solutions in TFE were added to a DMPC solution in methanol (1 mL; 12 mM) and vigorously vortexed. The solvent was removed by evaporation in a rotary evaporator. The mixed films were then dried for 24 h under vacuum. The films were hydrated in 0.5 mL of 10 mM ammonium acetate buffer (pH 7.5). Large unilamellar vesicles (LUVETs) were prepared by extrusion through a 200 nm filter. H/D exchange was initiated by diluting the LUVET suspensions 50 times in 20 mM ammonium acetate deuterated buffer (pD 7.5). The final concentration of the peptides was approximately 10 μM. When sodium-cationized species were studied, sodium iodide was added to a final concentration of 1 mM. At selected time points, 2 μL of this diluted suspension was transferred into a gold-coated glass capillary, and the measurement was started as quickly as possible. The dead time between dilution and measurement was 1 min.

**ESI MS Measurements.** ESI MS measurements were performed on a quadrupole time-of-flight instrument (Q-ToF; Micromass Ltd., Manchester, U.K.) operating in positive ion mode and equipped with a Z-spray nano-ESI source, or an LCQ ion trap instrument (ThermoQuest), equipped with a Protana source setup. Nano-ESI capillaries were prepared as described before.<sup>9</sup> The nano-ESI capillary was positioned approximately 5 mm before the orifice of the mass spectrometer. For MS experiments on the Q-ToF instrument, the quadrupole was set in the RF-only mode to act as an ion guide to efficiently link the ESI ion source with the reflectron time-of-flight analyzer. The potential between the nano-ESI capillary and the orifice of the mass spectrometer was typically set to 1.8 kV, and the cone voltage was set to 80 V. The source temperature was 80 °C. In MS/MS mode, the quadrupole was used to select precursor ions, which were fragmented in the hexapole collision cell, generating product ions that were subsequently mass analyzed by the orthogonal time-of-flight mass analyzer. For MS/MS measurements on the Q-ToF instrument, the collision energy was set to values between 80 and 100 V for sodiated

peptides, and between 40 and 60 V for protonated peptides. Argon was used as collision gas at a pressure of 25 psi. The quadrupole mass resolution parameters were set to a relatively large mass window to select the entire isotope envelope of the precursor ions. The reflectron time-of-flight parameters were set such that the fragment ions were detected at more than unit mass resolution, as required to obtain isotopically resolved (fragment) ion peaks.

For MS experiments on the LCQ, the capillary temperature was set to 150 °C. The capillary voltage and spray voltage were set to 20 V and 0.90–1.20 kV, respectively. The tube lens offset was 50 V. In the ion optics, the octapoles were set to –3.90 and –19.0 V, and the lens voltage was –40 V. The maximum injection time was chosen to be 1000 ms. For MS/MS measurements on the LCQ, the collision energy was set to 80% for Na<sup>+</sup>-cationized parent ions. The entire isotope envelope was selected for CID MS analysis.

**Deuterium Uptake Calculations.** The increases in deuterium content of the peptide fragments (in Da) were calculated by using the average mass-to-charge (*m/z*) values of the isotope clusters of the nondeuterated peptide (fragments) and the partly deuterated peptide (fragments), as described in more detail previously.<sup>9</sup>

## Results

**Global H/D Exchange Profiles.** Global H/D exchange profiles of the peptides given in Table 1 were determined to verify their incorporation in a transmembrane orientation in the phospholipid bilayer. These peptides vary primarily in the flanking residues (bold-faced in Table 1). Global H/D exchange of the transmembrane peptides was measured by diluting the vesicle dispersions 1:50 in buffered D<sub>2</sub>O. A mass spectrum obtained after introducing vesicles of KALP23/DMPC directly into a Q-ToF mass spectrometer (Figure 1) was dominated by intense signals of phospholipid monomers and small oligomers. Still the protonated, and to a lesser extent the sodiated, KALP23 was visible and isotopically resolved. The insert shows at the top the nondeuterated peptide ions and at the bottom the partly deuterated peptide ions following dilution of the vesicle dispersion in D<sub>2</sub>O.

All peptides investigated show a similar distinct exchange pattern when the number of protected hydrogens is plotted versus incubation time in D<sub>2</sub>O (Figure 2A). The fast initial global exchange of approximately 2/3 of all exchangeable hydrogen atoms for all vesicle-incorporated XALP peptides studied reveals that these hydrogens are easily accessible to the deuterated solvent. For all peptides, the deuterium uptake levels off after approximately 10 min, although there is still a substantial amount of exchangeable hydrogen atoms left. This indicates that the peptides have a protected part in which the hydrogens exchange only at extremely low rates. The number of protected amide hydrogens was found to be in agreement with the number of amino acid residues in the hydrophobic core of the peptide, as has been shown before for a somewhat shorter WALP peptide analog.<sup>9</sup> It is therefore believed that the region of the peptide that is well protected from H/D exchange must be embedded in the hydrophobic core of the bilayer (see Figure 2B). Moreover, additional protection from exchange could be caused by the involvement of these amide hydrogens in hydrogen bonding in the transmembrane α-helical structure.<sup>9,10</sup> Several complementary experiments confirm this hypothesis. Circular dichroism measurements have revealed that all WALP peptides and KALP23 (as well as FALP21, YALP21, and HALP23, unpublished data) are soluble in phosphatidylcholine

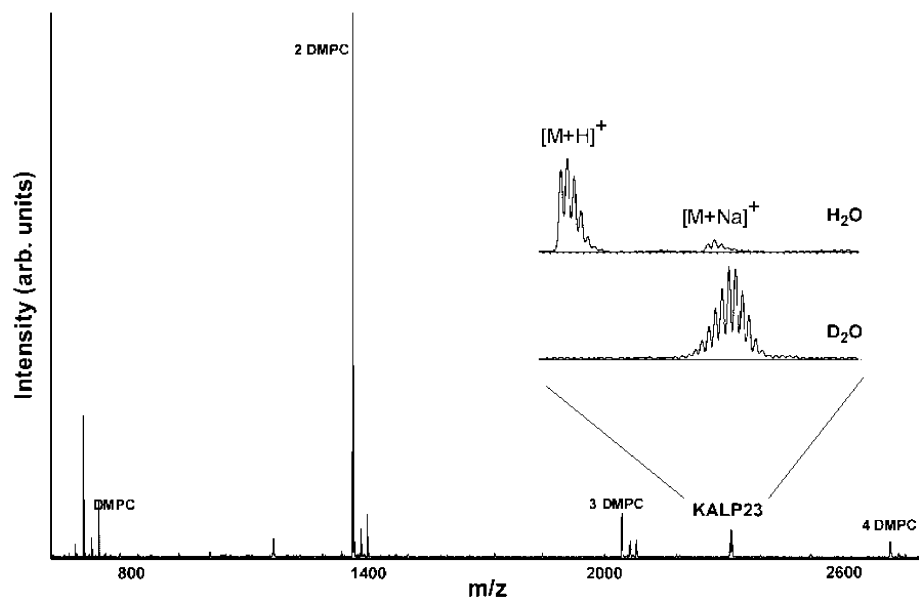


**Figure 1.** Mass spectrum obtained after introducing KALP23/DMPC vesicles (ratio 1:25) directly from ammonium acetate buffer solution (no extra sodium iodide added) into a Q-ToF mass spectrometer. The DMPC monomers, as well as dimers, trimers, and tetramers (2 DMPC, 3 DMPC, and 4 DMPC, respectively), are clearly visible. KALP23 is observed mainly as a protonated species ( $m/z$  2288), although some sodium ionized ions can be observed as well at  $m/z$  values 22 Da higher than the protonated species. The insert shows the nondeuterated peptide sprayed from vesicles dispersed in  $H_2O$  buffer, as well as the partly deuterated peptide sprayed from vesicles dispersed in  $D_2O$  buffer after an incubation time of 24 h. The mass increase was in this case about 25 Da.

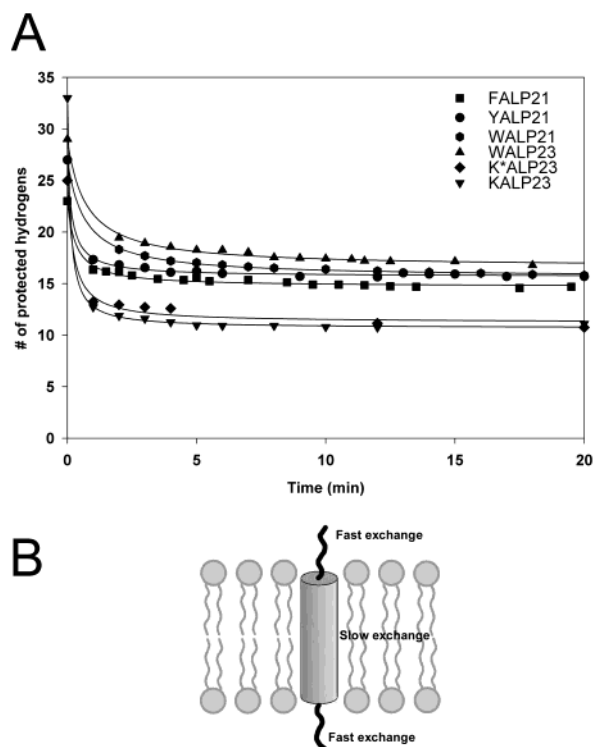


**Figure 2.** (A) Global H/D exchange curves of several transmembrane peptides. All peptides were reconstituted in phospholipid bilayers and subsequently incubated in  $D_2O$  buffer and sprayed directly from buffer solution. (B) Proposed incorporation model of transmembrane peptides in a phospholipid bilayer.

systems and form stable  $\alpha$ -helices.<sup>25</sup> The shorter protected region in KALP23 with respect to the other peptides can be explained by the different anchoring behavior of a lysine residue in the lipid bilayer headgroup region.<sup>24</sup>

Control experiments with fully deuterated peptides indicated that no back-exchange of either backbone or side-chain hydrogens took place during MS and MS/MS analysis.

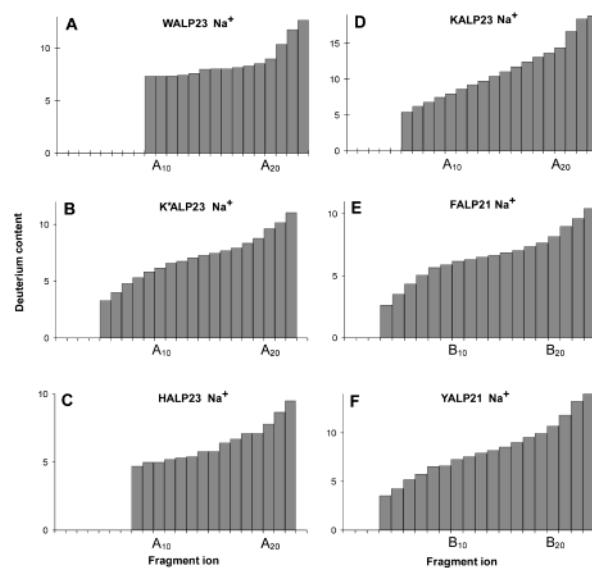


**Figure 3.** Deuterium content profiles of A fragment ions of partly deuterated sodium-cationized (A) WALP23, (B)  $K^*$ ALP23, (C) HALP23, (D) KALP23, (E) FALP21, (F) YALP21. Although only deuterium content profiles for the A ion series are shown here, the sodiated Y' fragment gave similar patterns.

### Effect of Selected Amino Acid Mutations on Deuterium Scrambling.

In our earlier work on WALP peptides, we showed by using CID MS that specifically the transmembrane parts of the peptides were protected from H/D exchange, as nearly no deuteriums were incorporated in these parts of the peptides.<sup>9,10</sup> To illustrate this further, Figure 3A shows the average deuterium content for all detected fragment ions of sodiated WALP23 precursor ions. In all experiments described in this section, CID MS was performed on the sodiated peptide ion, approximately 20 min after dilution in  $D_2O$ , allowing only easily accessible hydrogens to be exchanged. In the N-terminal A fragment ion series (for nomenclature, see ref 28) going from  $A_9$  to  $A_{20}$ , the

deuterium content increases only very little (plateau in the plot), suggesting that there is no significant deuterium uptake in the sequence region from Ala9–Leu20. The small increase in deuterium content might indicate (1) a very limited amount of scrambling, possibly involving the tryptophan side chains, or (2) a limited amount of H/D exchange in the peptide core. Because  $A_9$  was the smallest fragment ion observed in the CID MS spectrum, only information about the C-terminal part of the peptides could be derived from this fragment ion series. However, the complementary  $Y'$  fragment ion series gave similar information about the deuterium uptake in the N-terminal region (data not shown). The results in Figure 3D show the deuterium content profile for the A fragment ions of sodiated KALP23 precursor ions derived from CID MS experiments. In sharp contrast with the pattern for WALP23, the nearly linearly increasing curve suggests that the hydrogen and deuterium atoms have scrambled randomly over all available sites. For  $K^*$ ALP23 (Figure 3B), in which the lysine side chains were dimethylated, the deuterium content profile is quite different from that of KALP23. Instead of a random distribution of deuterium over the available sites as observed for KALP23, there is clearly a less steep gradient in the middle region of the diagram, indicating less deuterium incorporation in the transmembrane part. On the other hand, HALP23 (Figure 3C) and FALP21 (Figure 3E), like WALP23, seem to show a partly protected region. The plateau, however, is less pronounced than in the case of WALP23, revealing more scrambling in these cases. Finally, YALP21 shows a deuterium incorporation pattern resembling more KALP23 than WALP23.

The observations described here indicate that the scrambling is heavily dependent on the nature of the amino acid in the flanking residues. This dependence will be discussed in more detail below.

**Effect of Cationization on Deuterium Scrambling.** All data shown above were obtained from sodium-cationized peptides, because in general these hydrophobic peptides were rather difficult to protonate. To determine the influence of the nature of the charge carrier on the extent of scrambling, protonated as well as sodium-, potassium-, and cesium-cationized transmembrane peptides were subjected to CID MS. Both the  $[M + H]^+$  and the  $[M + Na]^+$  species of FALP21, HALP23, KALP23,  $K^*$ ALP23, and WALP23 could be generated and subjected to CID MS, although the spectra of the protonated ions of the latter two were of relatively poor quality because of low signal-to-noise ratios. In general, CID MS spectra of protonated species predominantly showed B and  $Y''$  ions, whereas the sodium-, potassium-, and cesium-cationized species gave rise primarily to A and  $Y'$  fragment ions (nomenclature according to ref 28).

In Figure 4, the resulting deuterium content profiles for the fragment ions of protonated WALP23,  $K^*$ ALP23, and HALP23 are given. The protonated ion pairs were generated from the same solution as the sodiated ones and studied under identical conditions, so they are directly comparable to the sodiated ones in Figure 3A–C. The bar diagrams indicate that there are clear differences in deuterium content profiles between CID fragments of protonated and sodium-cationized peptides. In general, fragmentation of sodium-cationized peptides results in profiles, indicating little deuterium uptake in the hydrophobic core. In contrast, CID MS on the complementary protonated peptides

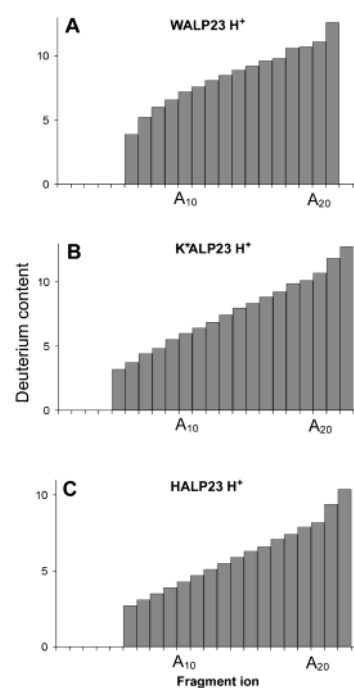


**Figure 4.** Deuterium content profiles of B fragment ions of partly deuterated protonated (A) WALP23, (B)  $K^*$ ALP23, (C) HALP23. Although only deuterium content profiles for the B ion series are shown here, the protonated  $Y''$  fragment gave similar patterns.

resulted in most cases in deuterium distributions randomly distributed over all exchangeable sites.

Even WALP23, which did not show much scrambling for the sodium-cationized species, shows a deuterium distribution pattern that indicates substantial scrambling when the protonated ions are studied. Also, the other protonated peptides showed a more random distribution of deuterium atoms over all exchangeable sites. Apparently, under the conditions used here fragmentation of protonated peptide ions does not result in deuterium profiles that are useful for the analysis of protected parts in the transmembrane peptide.

To investigate whether the sodium-cationized ion was unique in generating such deuterium profiles, or whether the size of the charge carrier also can influence the extent of scrambling, experiments were performed with potassium- and cesium-cationized peptide ions. Fragmentation of both  $K^+$ - and  $Cs^+$ -cationized HALP23, KALP23, and  $K^*$ ALP23 peptides resulted in the formation of mainly A and  $Y'$  fragment ions, comparable to  $Na^+$ -cationized species, although the amount of collision energy had to be increased. The deuterium patterns for  $K^+$ - and  $Cs^+$ -cationized peptides were similar to those of the  $Na^+$ -cationized peptides (data not shown).

**Effect of the Instrumental Setup on Deuterium Scrambling.** To study whether the observed behavior could be an artifact of the used instrument (Q-ToF), CID MS experiments on a representative set of sodiated WALP peptides were also performed on a LCQ ion trap. Not only is the interface different, but also the collisional activation process, including the reaction time, is somewhat different from the process as it occurs in the Q-ToF. Our data revealed that, in general, very similar deuterium uptake patterns could be extracted from the CID MS data taken on the hybrid Q-ToF and the LC-Q ion trap (data not shown).

Additionally, using the Q-ToF, in-source fragmentation experiments were performed as an alternative to CID MS in the

quadrupole collision cell. We performed these experiments to test whether the time window for ion fragmentation might have an influence on the observed deuterium scrambling. K\*ALP23 and WALP23 were measured using relatively high cone- and extraction voltages in the absence of collision gas. The disadvantage of this “nozzle-skimmer” dissociation is that there is no precursor ion selection. Still, the spectra recorded under these harsh conditions revealed many B and Y’ fragment ions of both K\*ALP23 and WALP23, indicating that mostly the  $[M + H]^+$  species of these peptide ions were fragmented. Although the signal-to-noise ratio was poor, the deuterium content plot obtained from these data showed a pattern similar to the one obtained from the protonated ions that were subjected to CID in the collision cell (data not shown).

## Discussion

### Comparison to Other H/D Exchange CID MS Studies.

H/D exchange in combination with gas-phase sequencing by CID MS of proteolytic peptide ions has become a frequently used method to probe structural properties of peptides and proteins.<sup>8,10,16,19–22</sup> The CID MS fragment ion data are used to resolve deuterium incorporation per amino acid in the protein. This interpretation of the CID MS data is only valid if deuterium scrambling prior to and during ion fragmentation can be excluded. In the present study, we have investigated parameters that influence the extent of deuterium scrambling in model transmembrane peptides. We do observe extensive scrambling, which seems to be in contrast to several of the above-mentioned studies. Therefore, we first consider some differences in experimental conditions between ours and the more conventional studies and the influence they may have on the scrambling process.

Solution-phase conditions, such as pH, temperature, and nature of the solvent, are important parameters in H/D exchange. In the conventional studies mentioned above, the peptide/protein sample is incubated in a buffered D<sub>2</sub>O solution at physiological pH. This is similar to our studies with the addition that the transmembrane peptides are now embedded in a phospholipid bilayer. In the analysis stage, in the conventional studies, pH and temperature drops (pH = 2–3, T = 0 °C) are introduced, which “freeze” the exchange (and/or back-exchange). We do not introduce such a step as our data reveal that after a few minutes of incubation the exchange rates in the lipid membrane environment are already close to zero. Therefore, the ionization process starts in our case from an aqueous solution at neutral pH, with the peptides embedded in the phospholipid bilayer. In the conventional studies, the peptide/protein ionization process starts from a cold, acidic, often aqueous/organic mixed solution. It cannot be excluded that these differences have an effect on possible H/D scrambling during the ionization process. As in our case, the ionization process is performed from a solution at a more physiological pH, and the rates for possible exchange are expected to be higher. Additionally, the presence of the phospholipid molecules may influence H/D scrambling during the ionization process. We should therefore be careful in directly comparing our results to those obtained in more conventional studies. Still, we envisage that scrambling mostly occurs in the gas phase during the activation and fragmentation step in the CID process. We note that extensive scrambling has been reported in some conventional studies as well for C-terminal

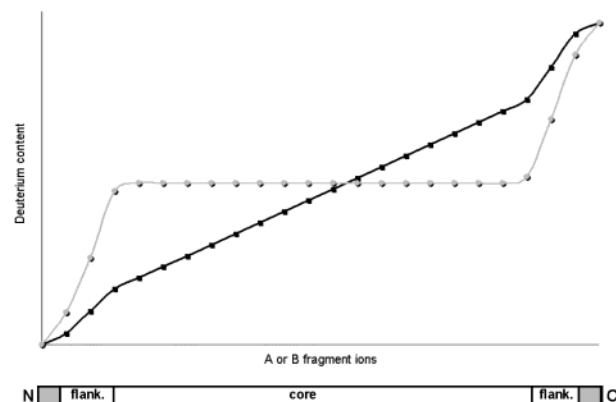


**Figure 5.** Schematic representation of the deuterium content in each fragment ion in the two limiting hypothetical cases of deuterium distribution over a 23-residue peptide, with flanking residues that have one exchangeable hydrogen in the side chain. The calculated deuterium content per fragment ions according to the *statistical state* model, in which full scrambling occurs, is depicted as a black line. The *core-protected* model, characterized by its slope of zero in the middle region, is represented by a gray line (see text for detailed description). For peptides with flanking amino acids that do not contain exchangeable hydrogens, the curves are somewhat different, and the calculations were adjusted.

ions,<sup>16,21,22</sup> albeit not for the complementary N-terminal ions. Our data reveal similar extents of scrambling for both types of ions. As the applied CID MS procedure is identical in all studies, we suggest that H/D scrambling is a process that should be properly addressed in all studies that combine H/D exchange with CID MS.

**Quantification of Deuterium Scrambling.** To quantify the extent of scrambling in our system, we define two limiting cases. In the first case, which we term the *statistical state*, the total deuterium content of the peptide is assumed to be statistically distributed over all available exchangeable sites in the peptide. This model therefore predicts that the subsequent fragment ions show a regular increase of deuterium content, which is only dependent on the number of exchangeable hydrogens present on each particular amino acid. The second limiting case we define as the *core-protected state*. In this model, we assume that the hydrophobic core region of the peptide is completely protected from exchange. In this *core-protected state*, the total number of deuterium atoms is first distributed over the terminal amino acids, which are not part of the inner hydrophobic core, whereas the remaining deuterium atoms are then added to the core region starting from the termini. This model would be in agreement with the expected positioning of transmembrane peptides in a lipid bilayer.

We can calculate the deuterium content for each peptide fragment generated by CID MS predicted by both models. This was done by taking a 23-residue peptide with one exchangeable hydrogen in its flanking-residues as an illustration. The resulting deuterium profiles are depicted schematically in Figure 5.

The results indicate that all experimental deuterium distributions of the different peptides can be classified using these limiting case models. When the patterns in Figure 3 are compared, it is evident that the deuterium distribution in the fragment ions of WALP23 follows to a large extent the core-protected state model, whereas the distribution for KALP23 closely follows the statistical state model.

For a more quantitative description of the extent of scrambling in the studied peptides, the deviations between the experimental

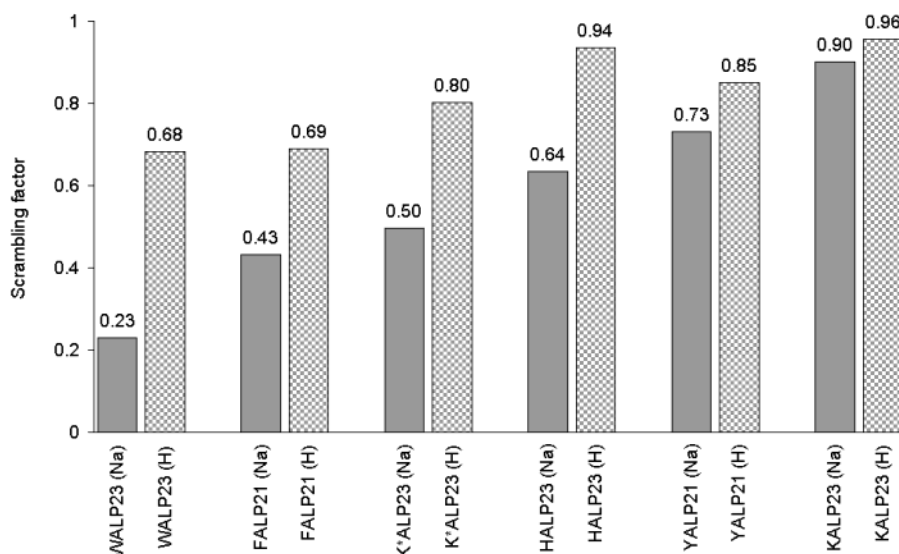


**Figure 6.** Scrambling factors for sodium-cationized and protonated peptides with variable flanking residues. The numbers were calculated using eq 1 with two extreme hypothetical cases as reference values (see text for details). Scrambling factors of sodium-cationized species are given as solid bars, and those of protonated species are given as block patterned bars.

and predicted deuterium content of the peptide fragments according to both models were compared using eq 1. From these deviations, a scrambling factor (SF) was determined for each different peptide ion.

$$\text{SF} = \frac{\sum_i^N |\Delta(D_{\text{st}} - D_{\text{co}})| - \sum_i^N |\Delta(D_{\text{st}} - D_{\text{ex}})|}{\sum_i^N |\Delta(D_{\text{st}} - D_{\text{co}})|} \quad (1)$$

In this formula,  $\Delta(D_{\text{st}} - D_{\text{co}})$  is the deviation between the deuterium content per fragment ion in the *statistical state* model and the *core-protected* model,  $\Delta(D_{\text{st}} - D_{\text{ex}})$  is the deviation between the deuterium content per fragment ion in the statistical state model and the experimental values,  $i$  is the individual subsequent fragment ions, and  $N$  is the total number of fragment peaks of which the mass increase could be determined from the CID MS spectra. The scrambling factor is thus defined as between 0 (indicating no scrambling) and 1 (representing a state with a statistical distribution of all deuterium atoms). The calculated scrambling factors are graphically shown in Figure 6, as a function of the charge carrier ( $\text{H}^+$  or  $\text{Na}^+$ ) and flanking amino acid. Some interesting features may be extracted from these data. The smallest scrambling factor observed is 0.23 for sodium-cationized WALP23. On the other end of the scale, protonated KALP23 reveals a scrambling factor of nearly 1. Of all transmembrane peptides studied here, these peptides represent the most extreme cases. From the calculated scrambling factors, it can be concluded not only that the variation in the charge carrier has a dramatic effect on the extent of deuterium scrambling, but also that different amino acids can induce various degrees of scrambling. This is in agreement with results reported by Buijs et al.<sup>15</sup> on the role of different amino acids on the extent of hydrogen migration in peptide ions. From the data presented, it can be concluded that the overall order of scrambling-inducing capacity of the studied flanking residues is the same for both the protonated and the sodium-cationized peptide ions, that is,  $\text{K} > \text{Y} > \text{H} > \text{K}^* > \text{F} > \text{W}$ .

**Table 2.** Gas-Phase Proton Affinity (According to Ref 35) and Number of Exchangeable Hydrogens for Each Flanking Amino Acid Residue

residue	gas-phase proton affinity (kcal/mol)	no. of exchangeable side-chain hydrogens
<b>H</b>	230.5	1
<b>K</b>	228.7	2
<b>W</b>	223.5	1
<b>Y</b>	220.7	1
<b>F</b>	219.9	0
<b>K*</b>	n.d.	0

The most direct indication that suggests the importance of the presence of exchangeable hydrogens at the flanking residues in the scrambling process comes from the substantial difference between sodium-cationized KALP23 ( $\text{SF}_{\text{Na}^+}$  0.90) and  $\text{K}^*\text{ALP23}$  ( $\text{SF}_{\text{Na}^+}$  0.50). However, as Phe does not have exchangeable side-chain hydrogens, this reasoning cannot be used to explain the observation that there is less scrambling in WALP23 ( $\text{SF}_{\text{Na}^+}$  0.23) than in FALP21 ( $\text{SF}_{\text{Na}^+}$  0.43). Moreover, significant differences are even observed between Trp-, His-, and Tyr-flanked transmembrane peptides, which all have one exchangeable side-chain hydrogen. Also, YALP21 ( $\text{SF}_{\text{Na}^+}$  0.73) showed more scrambling than both FALP21 and HALP23 ( $\text{SF}_{\text{Na}^+}$  0.64), although Tyr is more polar than Phe, and less polar than His. Therefore, the polarity of the amino acid cannot directly be correlated with the extent of scrambling. Also, there does not seem to be a direct relationship between the gas-phase proton affinity of the flanking residues and the extent of scrambling, because HALP23 and WALP23 have similar scrambling factors although their gas-phase proton affinities are quite different (see Table 2). Finally, the length of the hydrophobic stretch between the flanking residues does not seem to affect the amount of scrambling significantly, because a much longer KALP peptide (31 residues) revealed as much scrambling as KALP23 (not shown), and a shorter WALP peptide (16 residues) was similar to WALP23.<sup>9,10</sup>

The differences observed resulting from the different charge carriers are probably easier to interpret. The extent of scrambling seems to be highly dependent on the charge carrier being a

proton or an alkali metal ion. In all cases, fragmentation of the sodium-cationized species resulted in (far) less scrambling when compared to the protonated species. Interestingly, much more collision energy has to be transferred into the peptide ions to induce fragmentation in the sodium-cationized peptides when compared to the protonated species. The higher activation energy in sodium-cationized peptides does not seem to lead to an increase in the extent of scrambling. Our results suggest that the *less* activated protonated ions are more prone to hydrogen migration than are the *more* activated sodiated ions. We therefore hypothesize that in the gas phase the sodium ion is more fixed into a specific position, whereas the proton may more easily migrate between the different basic sites available in the peptide ion. This hypothesis is in agreement with the mobile proton model.<sup>29,30</sup> Our findings may suggest that the proton in the protonated species acts as a catalyst for deuterium scrambling.

Ion mobility studies<sup>31–33</sup> have revealed that gas-phase structures of ions may be very different from the solution-phase structures of their neutral counterparts and that they are highly dependent on the sequence of the peptides. For instance, in studies on poly-Ala derived peptides, the position of only one incorporated Lys residue spectacularly changed the gas-phase conformation.<sup>31,32</sup> On the other hand, peptide ion conformations in the gas phase are dependent on the nature of the charge carrier;<sup>13,34</sup> there are several indications that sodium-cationized peptides adopt in the gas phase a more compact structure than their protonated counterparts, which may render them less prone to hydrogen migration. We therefore propose that the observed trends in deuterium scrambling could be caused by differences

in gas-phase structures and energetics of the studied system. It is difficult to speculate about the possible structures the ions may adopt in the gas phase and about how these structures relate to the observed scrambling. To get a better view on this subject, it would be interesting to perform ion mobility studies on these ions, possibly in combination with theoretical structure and dynamics calculations.

## General Conclusion

The results obtained in this study indicate that intramolecular deuterium migration (scrambling) can occur during CID MS analysis. The extent of scrambling was found to be highly dependent on the nature of the charge carrier and the exact amino acid sequence, whereas it was independent of the type of mass spectrometer, as well as on the type of fragment ions studied. In general, alkali ion-cationized peptide ions revealed much less scrambling when compared to their protonated counterparts. It would therefore be advisable to implement this observation in structure and dynamics calculations. Moreover, the amino acid sequence of the peptide drastically influences the extent of deuterium scrambling, but it was difficult to correlate the observed trends directly to the molecular composition of the amino acid.

We conclude that although in general some detailed information on peptide and protein structural elements may be obtained by combining H/D exchange and CID MS, care has to be taken in the interpretation of the data as deuterium scrambling may influence the outcome of such measurements.

**Acknowledgment.** We would like to thank the Dutch Organization for Scientific Research (NWO; grant no. 700-97-011) for financial support. Drs. Roger E. Koeppe II and Denise Greathouse are acknowledged for synthesis of the WALP peptides. Dr. Claudia S. Maier is acknowledged for critically reading the manuscript.

JA0125927

- (29) Dongre, A. R.; Jones, J. L.; Somogyi, A.; Wysocki, V. H. *J. Am. Chem. Soc.* **1996**, *118*, 8365–74.
- (30) Wysocki, V. H.; Tsapralis, G.; Smith, L. L.; Brei, L. A. *J. Mass Spectrom.* **2000**, *35*, 1399–406.
- (31) Hudgins, R. R.; Ratner, M. A.; Jarrold, M. F. *J. Am. Chem. Soc.* **1998**, *120*, 12974–5.
- (32) Kinnear, B. S.; Hartings, M. R.; Jarrold, M. F. *J. Am. Chem. Soc.* **2001**, *123*, 5660–7.
- (33) Wyttenbach, T.; von Helden, G.; Bowers, M. T. *J. Am. Chem. Soc.* **1996**, *118*, 8355–64.
- (34) Reyzer, M. L.; Brodbelt, J. S. *J. Am. Soc. Mass Spectrom.* **2000**, *11*, 711–21.
- (35) Bojesen, G.; Breindahl, T. *J. Chem. Soc., Perkin Trans. 2* **1994**, 1029–37.